NeuroImage 141 (2016) 282–290

Contents lists available at ScienceDirect

NeuroImage

journal homepage: www.elsevier.com/locate/ynimg

Predicting the transition from normal aging to Alzheimer's disease: A statistical mechanistic evaluation of FDG-PET data

Marco Pagani [a,b,*], Alessandro Giuliani [c], Johanna Öberg [d], Andrea Chincarini [e], Silvia Morbelli [f], Andrea Brugnolo [g], Dario Arnaldi [g], Agnese Picco [g], Matteo Bauckneht [f], Ambra Buschiazzo [f], Gianmario Sambuceti [f], Flavio Nobili [g]

[a] Institute of Cognitive Sciences and Technologies, CNR, Rome, Italy
[b] Department of Nuclear Medicine, Karolinska Hospital Stockholm, Sweden
[c] Environment and Health Department. Istituto Superiore di Sanità, Rome, Italy
[d] Department of Hospital Physics, Karolinska Hospital, Stockholm, Sweden
[e] Istituto Nazionale di Fisica Nucleare, Sezione di Genova, Italy
[f] Department of Nuclear Medicine, Department of Health Science (DISSAL), University of Genoa and IRCCS AOU San Martino-IST, Genova, Italy
[g] Clinical Neurology, Department of Neuroscience (DINOGMI), University of Genoa and IRCCS AOU San Martino-IST, Genova, Italy

ARTICLE INFO

Article history:
Received 18 May 2016
Accepted 20 July 2016
Available online 22 July 2016

Keywords:
FDG-Pet
Normal aging
Mild cognitive impairment
Alzheimer's disease
Principal component analysis
Degree of order

ABSTRACT

The assessment of the degree of order of brain metabolism by means of a statistical mechanistic approach applied to FDG-PET, allowed us to characterize healthy subjects as well as patients with mild cognitive impairment and Alzheimer's Disease (AD). The intensity signals from 24 volumes of interest were submitted to principal component analysis (PCA) giving rise to a major first principal component whose eigenvalue was a reliable cumulative index of order. This index linearly decreased from 77 to 44% going from normal aging to AD patients with intermediate conditions between these values ($r = 0.96$, $p < 0.001$). Bootstrap analysis confirmed the statistical significance of the results.

The progressive detachment of different brain regions from the first component was assessed, allowing for a purely data driven reconstruction of already known maximally affected areas.

We demonstrated for the first time the reliability of a single global index of order in discriminating groups of cognitively impaired patients with different clinical outcome. The second relevant finding was the identification of clusters of regions relevant to AD pathology progressively separating from the first principal component through different stages of cognitive impairment, including patients cognitively impaired but not converted to AD. This paved the way to the quantitative assessment of the functional networking status in individual patients.

1. Introduction

Spontaneous neuronal activity in resting state depends on dynamic communication between brain regions resulting in both local segregation and long distance integration of neuronal processes. Several functional networks with temporally and/or spatially coherent connections (Damoiseaux et al., 2006) have been identified in healthy subjects by means of functional Magnetic Resonance Imaging (fMRI) and Positron Emission Tomography (PET). Brain connectivity has been assessed by investigating the mutual correlations between pre-determined volumes of interest (VOIs) (Huang et al., 2007; Nobili et al., 2008; Pagani et al., 2009; Wang et al., 2007), between a seed region and the whole brain (Gardner et al., 2014; Lee et al., 2008; Morbelli et al., 2012) or by the combination of the two (Seeley et al., 2009). Submitting all brain voxels to Independent Component Analysis has shown a strong functional architecture agreement in resting and activation states (Smith et al., 2009), dementia (Rombouts et al., 2009) and Amyotrophic Lateral Sclerosis (Pagani et al., 2016) speaking in favor of neuronal circuits constantly operating in healthy and pathological states.

The selective breakdown of intrinsic brain networks during the progression from the normal aging (NA) to mild cognitive impairment (MCI) and Alzheimer's Disease (AD) has been observed by different groups (Hahn et al., 2013; Liu et al., 2012; Sun et al., 2014; Wang et al., 2007). These investigations have already been performed, using fMRI approach, by other groups adopting complex network formalism by means of graph invariants (Bullmore and Sporns, 2009; Eguiluz et al., 2005). The analyzed graphs supporting both modularized and integrated information processing have brain areas as nodes, while the existence of an edge between two areas corresponds to the existence of a correlation between them, exceeding a pre-fixed threshold. More recently Spetsieris et al. have described by PET and Scaled Subprofile Model a longitudinal decay of default mode network in Parkinson's disease (Spetsieris et al., 2015).

http://dx.doi.org/10.1016/j.neuroimage.2016.07.043
1053-8119/

The disruption of neural pathways causing disconnection in large-scale brain organization has also been ascribed to the overall decrease in the number of fibers connecting brain structures, thus lowering the efficiency of information elaboration (Bozzali et al., 2011; Daianu et al., 2013) which is consistent with the worsening of cognitive symptoms. Such a process favors local systems to take over on long-distance brain connections and decreases intellectual abilities, (van den Heuvel et al., 2009) which lead to a hypothesis of a *continuum* in the intrinsic network degradation from normal aging to mild cognitive impairment to AD dementia.

The above described approaches focus on statistical comparisons between VOIs' pairwise correlations at different degrees of severity of the disease (Hahn et al., 2013) or, considering the between-area connectivity structure as a small-world network, concentrate on the effect of pathology on graph invariants such as characteristic length or node centrality (Liu et al., 2012). They do not include the possibility of extracting explicit state variables relative to the brain-as-a-whole.

On the other hand, a classical statistical mechanistic definition of system degree of order (Gorban et al., 2010), independent of any a priori hypothesis on the underlying architecture of the system under investigation, enables the transformation of a purely descriptive approach into a physically grounded one (Gorban et al., 2010; Mikulecky, 2001). This shift allows for both a quantitative definition of the amount of connectivity and a thorough analysis of the dynamics by which different areas lose contact with the main core of the functional network ('giant component' in the complex network jargon). Placing brain functional order dynamics in a statistical mechanistic perspective results in a characterization of the transition pattern of the system, possibly consistent with a progressive change typical of small-world connectivity (Scheffer et al., 2012).

The purpose of the present study was to analyze ^{18}F-Fluorodeoxyglucose PET (FDG-PET) data by a statistical mechanistic approach in order to characterize the degree of order dynamics across normal aging, subjects with MCI either converting to AD (early MCI, eMCI, and late MCI, lMCI) or not (ncMCI), and patients with mild AD dementia. This was made possible by quantifying the progressive disruption of the main core network present in normal aging and by identifying those brain regions in which such global disconnection was more pronounced. We also checked the clinical relevance of our theoretical physics-inspired model by a bootstrap approach comparing the percentage of the variation explained by the first principal component across the different groups.

The degree of correlation of the brain as a whole gives much more robust results than single areas/nodes evaluations. This depends upon the acceptance of the ergodic hypothesis that could, in principle, provide the basis for direct evaluations of the degree of order of brain metabolism at the single patient level. In turn, this translates into the assumption that patients inside a clinical class of severity are equivalent to a single patient observed during different times within a stationary clinical state. This implies that the degree-of-order we measure across patients of the same class is equivalent to that derived from different time points of the same patient. In turn, this could provide a rapid and efficient prognostic system for 'time-to-onset' of AD.

2. Methods

2.1. Participants

Two hundred and twenty subjects composed the whole study population. They were 44 normal aged subjects (NA; mean age 69 ± 10; 32 Females), 28 MCI patients not converting to AD at 5 years follow up after PET scan (not converting MCI, ncMCI; mean age 72 ± 6; 12 Females), 36 MCI patients that converted to AD later than 2 years since PET scan (early MCI, eMCI; mean age 75 ± 7; 28 Females), 58 MCI patients that converted to AD within 2 years since PET scan (late MCI, lMCI; mean age 76 ± 7; 36 Females) and 54 patients with mild AD dementia at the time of PET scan (AD; mean age 73 ± 7; 36 Females). These patients come from a prospective study started in 2008 including patients with amnestic MCI, after secondary causes of deficit were excluded, and patients with mild AD dementia, who gave their consent to undergo FDG-PET in the frame of a long-term observational study. They all provided informed consent to be part of a longitudinally followed cohort.

Although the proposed definition of eMCI and lMCI was based on the Standard Deviation (SD) from norms (i.e., lower than −1.5 SD = lMCI; between −1.0 and −1.5 = eMCI) (Aisen et al., 2010) we choose a temporal-based classification by defining as eMCI those patients converting to AD dementia more than 2 years later the first visit and lMCI those converting before this timeline. Actually the terms 'early' and 'late' (stage) essentially should refer to a temporal rather than to a neuropsychological test score domain.

2.1.1. MCI patients

They were subjects referred to our memory clinic for a first diagnostic assessment of a memory complaint. They underwent a complete diagnostic work-up according to current standards, including clinical and neuropsychological examinations, blood and urine tests, morphological (MRI) and functional (FDG-PET) neuroimaging. Patients underwent a neuropsychological test battery, including: (i) categorical and phonological verbal fluency; (ii) Trailmaking test A and B and Stroop color and color-word test for executive functions; (iii) figure copying of the mental deterioration battery (simple copy and copy with guiding landmarks) and Clock Completion test to assess visuospatial abilities; (iv) Rey Auditory Verbal Memory Test (RAVLT, immediate and delayed recall) and Corsi's block design to investigate memory; (v) digit span (forward) and symbol-digit to asses attention and working memory.

To be included in the MCI group the patients had to be impaired in a memory test, either with (multi-domain amnestic MCI) or without (single-domain amnestic MCI) impairment in other cognitive domains but not demented, thus corresponding to the Petersen's MCI criteria (Petersen and Negash, 2008). Moreover, they must be followed-up with regular control visit at least for 5 years or until they developed AD dementia. Exclusion criteria included previous or current major psychiatric disorder and neurological disease, severe and uncontrolled arterial hypertension, diabetes mellitus, renal, hepatic or respiratory failure, anaemia and malignancy. A depressive trait was not an exclusion criterion, but a 15-item Geriatric Depression Scale (GDS) score ≤ 10 was required for inclusion. Patients with MRI evidence of major stroke or brain mass were excluded, with white matter hyperintensities, leucoaraiosis and lacunae not constituting an exclusion criterion if the Wahlund score was <3 in all regions(Wahlund et al., 2001). The modified Hachinski ischaemic score (Loeb and Gandolfo, 1983) was lower than 3 in all patients. Patients fitting the criteria for vascular cognitive impairment (Gorelick et al., 2011) were excluded. A subgroup of patients who did not undergo MRI because of claustrophobia or the presence of a metallic device were evaluated by Computed Tomography.

2.1.2. AD patients

Similar as MCI patients, these were patients at their first diagnostic evaluation at our memory clinic, who were diagnosed as affected by mild AD dementia at the end of the same diagnostic procedure applied to MCI patients. The presence of dementia was established by clinical interview with the patient and informants, using the questionnaires for activities of daily living (ADL), instrumental ADL (IADL), and the Clinical Dementia Rating (CDR) scale. The Mini-Mental State Examination (MMSE) was used to assess general cognition. Only patients with mild dementia (i.e. with MMSE score ≥ 19) attributed to AD according to the NIAAA criteria (McKhann et al., 2011) were included.

2.1.3. Controls

The control subjects were healthy volunteers who gave their informed consent to participate to the study. Their healthy condition

was carefully checked by means of general medical history, clinical examination, and the same exclusion criteria as for patients, with the exception of cognitive complaints. MMSE was performed, and only subjects with a normal score (i.e., >26) were considered. Moreover, only subjects with a CDR of 0 were included. These subjects underwent FDG-PET and MRI. Given these prerequisites, the control subjects were chosen with the selection criteria of being in the same age range, having similar gender distribution and educational level as patients.

All subjects underwent the same neuropsychological test battery including standard tests for attention, language, visuoconstruction, and executive function in use in our laboratory. A *Z*-score lower than −1.5, computed on the Italian normative values of each test and corrected for age and education, was established for impairment in a specific cognitive domain (Picco et al., 2014).

2.2. ^{18}F-FDG PET protocol and preprocessing

FDG-PET was acquired according to the guidelines of the European Association of Nuclear Medicine (Varrone et al., 2009). Briefly, subjects fasted for at least 6 h. Before radiopharmaceutical injection, blood glucose was checked and was <7.8 mmol/l in all cases. After 10 min rest in a silent and obscured room, with eyes closed and ears unplugged, subjects were injected with approximately 200 MBq of ^{18}F-FDG via a venous cannula. They remained in the room for 30 min after the injection and then moved to the PET room where scanning started approximately 45 min after the injection. A polycarbonate head holder was used to reduce head movements during the scan. Images were acquired by means of a SIEMENS Biograph 16 PET/CT equipment with a total axial field of view of 15 cm and no interplane gap space. Scan acquisition time was 15 min with 3-dimensional mode. Images were reconstructed through an ordered subset-expectation maximization algorithm, 16 subset and 6 iterations, with a reconstructed voxel size of 1.33 × 1.33 × 2.00 mm. Attenuation correction was based on CT scan. Dicom files were exported and converted into Analyse files.

FDG-PET images were subjected to affine and nonlinear spatial normalization into the Talairach and Tournoux's space using SPM8 (Wellcome Department of Cognitive Neurology, London, UK) implemented in Matlab 7.5 (Mathworks, Natick, Massachusetts, USA). The spatially normalized set of images was then smoothed with a 10-mm isotropic Gaussian filter to blur individual variations in gyral anatomy and to increase the signal-to-noise ratio. All the default choices of SPM8 were followed with the exception of spatial normalization for which the $H_2^{15}O$ template was replaced by a customized brain FDG-PET one (Della Rosa et al., 2014).

2.3. Region of interest identification and data preprocessing

Mean metabolic values were computed in 45 anatomical volumes of interest (VOIs) in each hemisphere (90 VOIs) as defined by the AAL Atlas (Tzourio-Mazoyer et al., 2002). An in-house created Matlab-based script automatically processed mean FDG uptake from each of the 90 VOIs (Pagani et al., 2015). Within each subject VOIs were normalized to the average intensity of the cerebellar one, known to be poorly affected by AD pathology. Regions with similar anatomo-functional characteristics were further merged into meta-VOIs in order to decrease the number of variables to be submitted to statistical analysis. The computations were performed by the Matlab script in a single step lasting a few minutes, rendering simple and friendly the whole process.

Twelve meta-VOIs were constructed in each hemisphere: 1. Occiptal Cortex (Calcarine/Lingual/Inferior Occipital/Middle Occipital/Superior Occipital Gyri); 2. Thalamus/Putamen/Pallidum/Caudate; 3. Parahippocampal gyrus/Amygdala/Hippocampus/Insula; 4. Orbitofrontal Cortex (Inferior Frontal/Medial Frontal/Middle Frontal Gyri); 5. Frontal Cortex (Middle Frontal/Superior Frontal/Superior-Medial Frontal/Superior-Orbital Frontal/Inferior Frontal Gyri); 6. Cuneus/Fusiform Gyrus/Precuneus; 7. Postcentral Gyrus/Precentral Gyrus/Supplementary Motor Area; 8. Parietal Lobe (Inferior Parietal/Superior Parietal Gyri); 9. Anterior Cingulate Gyrus, 10. Posterior Cingulate Gyrus, 11. Temporal Lobe (Inferior Temporal/Middle Temporal/Superior Temporal Gyri), 12. Temporal Pole (Middle Temporal Pole/Superior Temporal Pole Gyri).

We also tested another anatomical parcellation (35 VOIs, bilaterally, from the Wake Forrest University, WFU, Pick Atlas) besides the AAL Atlas, to verify that results were not dependent on the initial VOI choices, obtaining highly consistent results.

2.4. General theoretical frame, methods and strategy of analysis

The degree of order is a state variable largely used for the characterization of systems dynamics (Chandler, 1987) defined as the amount of internal correlation. Any system has a peculiar behavior of decreasing (or increasing) its degree of order when stressed by an external force. This behavior, depending on the particular structural features of the system, can take the form of either an abrupt transition or a smooth decay, corresponding the latter to a trajectory optimally fitted by a straight line. A well-studied and clear example of the above two alternative behaviors is the folding process of protein molecules that can be subdivided into two-state (abrupt transition) and multi-state (quasi-linear dynamics) (Tan et al., 1996).

Gorban et al. (Gorban et al., 2010) and more recently Scheffer et al. (Scheffer et al., 2012) demonstrated the universal character of such dynamics ranging from physics to physiology and economics. Heterogeneous networks in which the components differ and where incomplete connectivity causes modularity tend to have adaptive capacity in that they adjust gradually to changes. All such cases result into a smooth degradation of the network when stressed by an external factor. By contrast, in highly connected and homogenous networks, local losses tend to be repaired by subsidiary inputs from linked units until at a critical stress level the system collapses (Scheffer et al., 2012).

This ends up into two main classes of degradation (i.e. loss of order) of networks, strictly depending on their wiring architecture. Highly modular and heterogeneous networks (nodes with highly varying connectivity degree) show a smooth degradation, while highly connected homogeneous networks undergo sharp transitions.

The construction of a synthetic measure of the degree of order of the brain as a whole was straightforward in the case of FDG-PET data. For each clinical severity level, principal component analysis (PCA on the correlation matrix) was applied to the data set having as statistical units the patients and as variables the mean intensity in the meta-VOIs. The analysis was performed separately for each severity group. All different groups had the same correlation structure characterized by a main first principal axis acting as 'size' component (all positive loadings, thus representing the behavior of the brain as a whole) (Darroch and Mosimann, 1985; Jolicoeur and Mosimann, 1960). This allowed for a direct quantification of the degree of order of the brain in terms of the first eigenvalue (Lambda 1) of the PCA solution expressed in terms of percentage of total variance explained by the first principal component (Giuliani et al., 2001; Gorban et al., 2010). The formal identity between the amount of correlation and the degree of order of a system derives from the mathematical definition of algorithmic complexity (Soofi, 1994). The invariance of degree of order dynamics at different brain partition choices is demonstrated in Suppl. Fig. 1, where both the strict correlation between degree of order of VOI and meta-VOI (top panel) and their collinear decrease across disease severity (bottom panels) are reported.

The detachment of brain areas from the global connectivity component was evaluated by Oblique Principal Component Analysis (OPC) (Jolliffe, 2002; Sethi, 1971) as applied to all meta-VOIs loadings on the first principal component of PET data of the different groups of patients.

OPC is a divisive clustering procedure for variables. The variables (in our case, the brain areas loadings on PC1 of groups with increasing severity) are subdivided into classes with the constraints of obtaining

most internally correlated clusters (maximal correlation between variables within the same cluster) while at the same time minimizing the between-cluster correlation (minimal correlation among variables pertaining to different clusters). The procedure stops when reaching a maximum of the ratio between the within-cluster and the between-cluster correlation. The composition of different clusters of meta-VOI was checked *a posteriori*: the presence of well-known AD affected areas in rapid decay cluster (areas whose loading starts to decrease already at ncMCI stage) is a proof-of-concept of the biological relevance of the obtained partition. Data inspected by OPC do not explicitly contain information about the entity of the metabolism in different areas. The loadings correspond to the correlation coefficient between the areas and PC1, thus they estimate the degree of integration of each area with global brain metabolism.

Each loading derives from the group specific PCA. Given that we have 5 disease severity groups, each area is defined by 5 values, each one correspondent to its loading with PC1 of the specific group. This allows to have a consistent representation of each area in terms of its participation to PC1 across the 5 severity classes. OPC collects in the same class areas having the same PC1 loading profile across the 5 classes.

We supplemented the analyses by computing a confidence level estimation with the bootstrap technique on the degree of order for each clinical class. This allowed for an assessment of discrimination power among different cognitive severity classes which might cross-check the clinical relevance of our physical model. It is worth stressing the mutual independence between Bootstrap analysis (only based on Lambda 1) and OPC partition that constitutes a global descriptive analysis of the contribution of the various clusters of areas to PC1.

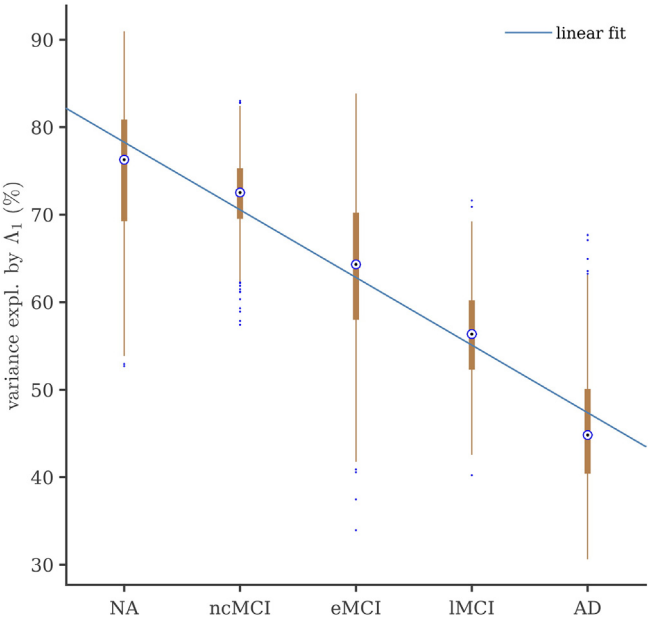

Fig. 1. The dynamics of the loss of order along the clinical status. Y-axis: variance explained by the first component; X-axis: disease severity. NA: normal aging; ncMCI: MCI patients not converting to AD at 5 years follow up; eMCI: MCI patients that converted to AD later than 2 years; lMCI: MCI patients that converted to AD within 2 years; AD: patients with mild AD dementia. The point distribution around the center of mass corresponds to bootstrap simulation.

3. Results

3.1. Order degree dynamics

Submitting to PCA the intensity values of the 24 meta-VOIs estimated for each subject of the five groups of our dataset and computing the eigenvalue of the first component of each group (Lambda 1), resulted in the dynamics shown in Fig. 1. The linear decay of the degree of order (percentage of variance explained by the first component) is consistent with a highly modular architecture of brain metabolism (Scheffer et al., 2012). The percentage of total variance explained by the first principal component was 77.08 in NA, 71.00 in ncMCI, 64.08 in eMCI, 54.97 in lMCI and 44.01 in AD, $r = 0.96$, $p < 0.001$.

The dynamics of Lambda 1 on simple VOIs (not aggregated in meta-VOIs) show the same monotonic behavior of degree of order irrespective of the initial preprocessing (Supplementary Fig. 1). Using the functional parcellation of the WFU Pick Atlas resulted in dynamics superimposable to the analyses performed using AAL for segmenting both VOIs and meta-VOIs.

3.2. Oblique principal component (OPC) analysis

OPC, applied to the distribution of brain areas on the first principal component in different groups of patients, generated a five-Cluster partition of the meta-VOIs set as the optimal classification. This partition explained 91% of the total variance. Thus, it can be considered a faithful representation of the different patterns of loading decline across stress variable. Table 1a reports the composition of different Clusters in terms of meta-VOIs and reports the centrality of each area with its own Cluster in terms of R-square. The two most populated classes (Clusters 1 and 4) were largely superimposed (Inter-Cluster correlation = 0.88), which indicates largely coincident loading dynamics (Table 1b).

The profiles of loadings within the first component for different Clusters are reported in Fig. 2 and their topographic representation on brain surface in Fig. 3a and b. It should be stressed that the observed Cluster structure emerged from a purely data-driven mode based solely on the loading of single meta-VOIs on the first component relative to each disease severity class.

Clusters 1 and 4 correspond to meta-VOIs whose detachment from the main component (whole brain metabolism) follows a smooth decay along the axis of increasing severity (Fig. 2). Cluster 1 containing most of the typical regions of the Alzheimer hypometabolic pattern (Table 1a), has its lowest load on Principal Component 1 (PC1) in AD patients while MCI patients of all groups, including ncMCI show a similar loading. In other words, Cluster 1 distinguishes AD dementia from predementia AD. On the other hand, Cluster 4, including some of the main association cortices, depicts the transition across several stages of AD severity with a high linearity since loading progressively decreases with cognitive decay.

Clusters 2 and 5 were closely related to global brain metabolism throughout the entire dynamics, while cluster 3 points to areas with a highly non-linear loading dynamics.

3.3. Consistency between brain metabolism ordering and diagnosis

The last step of the analysis was to check the ability of degree of order to account for the clinical differences between the severity classes. The data set was analyzed by a bootstrap procedure to estimate the variability of Lambda 1. The estimated discrimination power of Lambda 1 (Fig. 4) indicates that the degree-of-order metric has strong potential for being considered a clinical indicator since the Area Under the Curve (AUC) differentiating ncMCI from the other groups was 64% for NA, 84% for eMCI, 98% for lMCI and 100% for AD.

4. Discussion

The study presents robust evidence, analyzing the progressive disruption of the main core network present in normal aging, that the metabolic structure of the brain loses its connectivity during the transition to mild AD. This decay from a high to a low degree of order is progressive and strongly correlated with clinical severity, ranging from a

Table 1a
The most detailed (maximal number of Clusters) classification of brain areas in terms of their dynamics of relation with the 'giant component' of brain metabolism as such. The clustering procedure halts when a further subdivision generates too near (i.e. too correlated each other) Clusters to be discriminated. R-square is a measure of each area centrality with respect to its own Cluster, the greater the R-square, the greater the centrality of the area.

Cluster 1		Cluster 2		Cluster 3		Cluster 4		Cluster 5	
Meta-VOI	R^2	Meta-VOI	R^2	Meta-VOI	R^2	Meta-VOI	R^2	Meta-VOI	R^2
AMY_HIPPO_INS_L	0.9731	CINGULATE_L	0.8498	PAL_CAU_PUT_R	0.7466	OCCIPITAL_L	0.9092	FRONTAL_L	0.9876
AMY_HIPPO_INS_R	0.9525	THALAMUS_L	0.8856	PRE_POST_CENTR_L	0.7466	OCCIPITAL_R	0.9549	FRONTAL_R	0.9876
CUN_PRE_CUN_FUS_L	0.9443	THALAMUS_R	0.7621			PAL_CAU_PUT_L	0.9155		
CUN_PRE_CUN_FUS_R	0.9678					ORBITO_FRONTAL_L	0.9498		
PRE_POST_CENTR_R	0.8510					ORBITO_FRONTAL_R	0.9326		
PARIETAL_R	0.9942					PARIETAL_L	0.9700		
CINGULATE_R	0.8759					TEMPORAL_L	0.9067		
TEMPORAL_POLE_L	0.9143					TEMPORAL_R	0.9242		
TEMPORAL_POLE_R	0.9577								

percentage of variance explained by the giant component of the correlation network of 77% in normal aging to 44% in mild AD dementia. The dramatic loss of order along the cognition severity transition is strictly monotonic (Pearson $r = 0.96$), pointing to a highly modular architecture of brain connection networks. The first step in the decay of order takes place between NA and the states of heterogeneous causes of cognitive deficit but that do not progress to dementia. The most obvious and probably the most frequent of those causes is moderate cerebrovascular disease that is not severe enough to fit the criteria for Vascular Cognitive Impairment but that together with other co-factors (such as drug therapy, chronic systemic diseases, low education, masked depression) may be enough to impair the brain metabolic connectivity compared to NA.

Patients that converted to mild AD at different times following PET examination had a decreasing degree of order. This suggested that their metabolic status at the time of PET was predictive of conversion, which was largely irrespective of the time occurred. This also implies that any perceived abrupt transition in patient clinical status does not depend on a change in an underlying singularity in brain metabolism connectivity but is rather a consequence of reaching a threshold value by a substantially constant decay. This constant connectivity decay rate must be interpreted as a gross average over the whole set of brain areas. To examine more in detail whether this caused a detachment from global brain metabolism of specific areas we applied OPC to loading dynamics of different brain areas.

The loss of global connectivity during the transition from NA to AD is an index of decline of the integration between different brain regions present at NA. Such decay is likely proportional to the progress of the pathological spreading of AD and speaks in favor of a higher anatomo-functional segmentation upon neurodegeneration leading to modules scarcely correlated with each other. In this respect, the loading profile of Cluster 1 containing most of the classical brain regions pertaining to the AD hypometabolic pattern (precuneus, cingulate cortex, medial temporal lobe structures) clearly separated AD dementia from all MCI stages and the latter from NA. As such, these regions are confirmed to be able to reveal the metabolic aspects of AD pathology, and are more involved in overt dementia, but they are unable to show the progression of the severity of damage until time to conversion. It is likely that the mechanisms leading to hypometabolism in these areas are already active while the cognitive symptoms appear to decline only later in the course of disease.

Cluster 4 showed a different behavior as it progressively lost its correlation with the giant component across all subject groups. It includes most association cortices, bilateral occipital, orbitofrontal, temporal cortex and left parietal cortex. Most of these areas are not strictly included in the AD signature but their metabolic/perfusion levels correlate to various extents with the neuropsychological decline in MCI as well as in AD patients (Nobili et al., 2005; Nobili et al., 2008). Therefore these areas are expected to show a more linear relationship with the advancing severity of disease and to be good markers of disease progression. These association cortical areas can also be affected by hypometabolism in other neurodegenerative diseases, such as frontotemporal dementia (Caroppo et al., 2015), dementia with Lewy bodies (Ishii et al., 2007) and Amyotrophic Lateral Sclerosis (Pagani et al., 2014).

The presence of thalamus in Cluster 2 could be unexpected as thalamic hypometabolism is not an usual finding in early AD patients.

Table 1b
Between Cluster Pearson correlation coefficients. Cluster 1 and Cluster 4 that are both monotonically decreasing their loading along disease severity are very correlated each other.

Cluster	1	2	3	4	5
1	1.00000	0.20550	−0.30464	0.87784	0.48373
2	0.20550	1.00000	−0.05450	0.60614	0.47501
3	−0.30464	−0.05450	1.00000	−0.12159	−0.37934
4	0.87784	0.60614	−0.12159	1.00000	0.65450
5	0.48373	0.47501	−0.37934	0.65450	1.00000

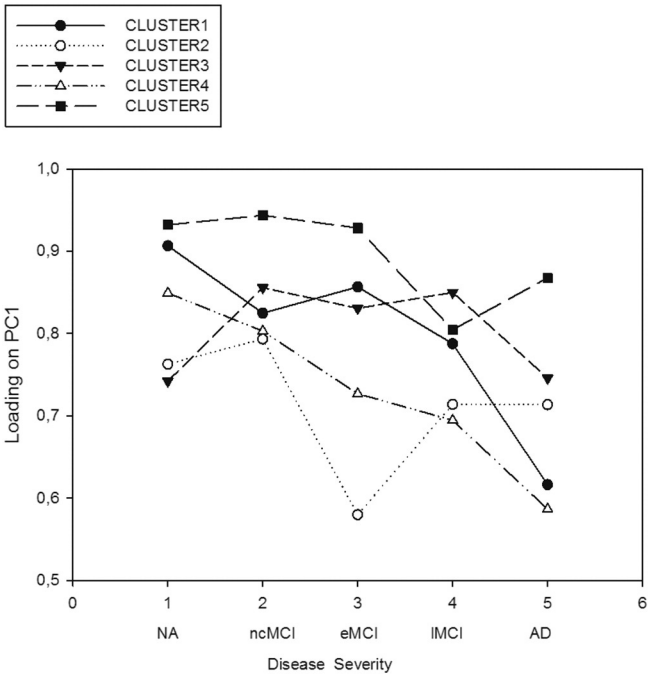

Fig. 2. Graphical depiction the profile of each Cluster in terms of loading dynamics. Y-axis: loading on the first principal component; X-axis: disease severity. NA: normal aging; ncMCI: MCI patients not converting to AD at 5 years follow up; eMCI: MCI patients that converted to AD later than 2 years; lMCI: MCI patients that converted to AD within 2 years; AD: patients with mild AD dementia.

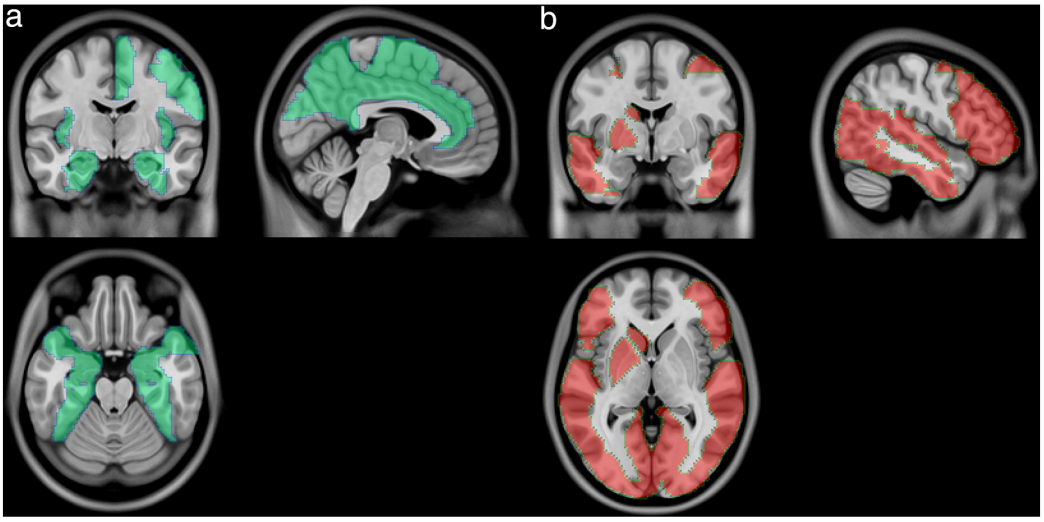

Fig. 3. Topographic representation of Cluster 1 (a) and Cluster 4 (b) on brain surface. The AAL regions corresponding to Cluster 1 and Cluster 4 (see Table 1a) have been superimposed to the Montreal Neurological Institute template in the coronal (top left), sagittal (top right) and transversal (bottom) views.

However, the thalamus is affected by relevant atrophy in AD (Canu et al., 2011; Yi et al., 2016), paralleling hippocampal atrophy (Stepan-Buksakowska et al., 2014). Moreover, thalamic hypometabolism could also result, at least partially, from partial volume effect.

Our results are consistent with several previous investigations performed by fMRI in which the highly interconnected networks have been assessed in the healthy state and in AD by a graph analysis whose basic theoretical paradigm is the small-world wiring architecture(Boccaletti et al., 2006; Sun et al., 2014). This paradigm roughly corresponds to graphs in which the shortest path length (the minimum number of edges to be traversed for connecting two nodes) is minimized by the contemporary presence of a strong modularity (domains made by areas more strongly connected among them than with areas pertaining to other modules) and high-betweeness nodes connecting different domains (Boccaletti et al., 2006).

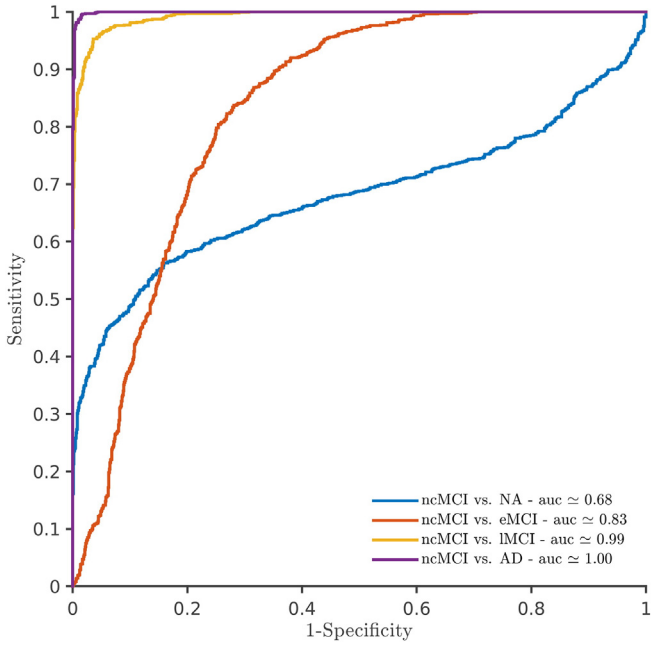

Fig. 4. ROC curves for NA (blue), eMCI (red), lMCI (yellow) and AD (violet) versus ncMCI. Both curves and areas under the curves (AUC) are estimates computed on bootstrapped distributions. NA: normal aging; ncMCI: MCI patients not converting to AD at 5 years follow up; eMCI: MCI patients that converted to AD later than 2 years; lMCI: MCI patients that converted to AD within 2 years; AD: patients with mild AD dementia.

The present approach allowed us to go deeply into in the phenomenon of connectivity loss from both a theoretical and a pathophysiological perspective. The presence of a leading component explaining the 77% of total variance of FDG-PET in normal aging and decreasing to 44% in mild AD is a proof of the possibility to unequivocally define the degree of order of the brain-as-a-whole by a single measure.

It is worth noting that all areas have positive and near-to-unit loadings with PC1: this points to the character of 'global statistical measure' of brain metabolism integration of PC1 eigenvalue. On the contrary, minor components have both positive and negative loadings so indicating relatively minor differential balances for specific local circuits. Since components are each other orthogonal by construction, a 'general' brain metabolic tone (PC1) goes hand-in-hand with local correlation circuits (minor components). The great majority of network analyses of brain metabolism deals with local circuits; the main novelty of our work is to focus on the 'global mode' (PC1).

This not only allowed for an easier development of quantitative (and robust) indexes potentially useful in early diagnosis with respect to the plethora of local between-ROIs pairwise correlations, as in graph analysis, but in principle paves the road for a physics-inspired approach to every disease for which a brain FDG-PET examination is clinically appropriate. The possibility to define a suitable degree-of-order as synthetic descriptor in other pathophysiological conditions could allow a fine monitoring of disease evolution in other fields of medicine. Furthermore the very large AUC areas, in particular those between ncMCI and eMCI and between ncMCI and lMCI confirm both the sensitivity of our analysis to detect subtle disruption of the brain networks and the consistency of the correlation of a FDG-PET pattern with the time needed to develop AD when at the MCI stage.

The present investigation introduces two novelties in brain networking research on AD. This is the first time in which a global network analysis on a heterogeneous population of MCI and AD patients is performed by FDG-PET. This is consistent with the work of Friston et al. (Friston et al., 1993) reporting an analysis on six normal subjects in which the first component accounted for 71% of total variance, very close to the 77% found in normal aging in the present study. Such agreement is even more remarkable if we consider that Friston's results

originated from an analysis performed on 500.000 voxels considered as single variables. Unlike fMRI, in which the input data are variations of signal during time with a resolution of a few seconds, metabolic analysis using cross-sectional FDG-PET data is based on patients' data in which each image represents the mean metabolic activity recorded from a single subject during about 30 min. of tracer uptake. The different nature of the input signals results in a conceptual difference between the networks extracted using fMRI and FDG-PET. The interregional correlations found by fMRI involve dynamic functional connections being basically time-driven with the meaning of temporal inter-correlations defined as temporal coherence between the low-frequency (<0.1 Hz) signal of spatially remote brain regions. Furthermore, fMRI-based networking which mainly reflects blood flow distributions might result in different patterns when investigated by FDG-PET (Di et al., 2012). Neurodegenerative processes integrate activity in networks, rather than in isolated regions. In AD as well as in other neurodegenerative disorders, long-distance interregional metabolic correlations between brain regions are impaired by the degeneration of neurons and white matter fibers (Fischer et al., 2015; Sorg et al., 2007). Such disengagement involves spatially connected synaptic activities that are affected by common pathophysiological processes which appear in two or more regions, possibly due to misfolded protein propagation across structural pathways (Iturria-Medina and Evans, 2015). The reorganization of reciprocal connections implies that local compensatory networks take over, increasing the anatomical and functional segregation of brain processes, which seems to be confirmed by our results of higher modularity during the course of the disease. FDG-PET, investigating metabolic spatial connectivity, captured the distributed regional networks built on anatomical and functional similarities specific to the progressive conversion from MCI to AD, beyond the low-frequency similarities between short-time local perfusion correlations disclosed by fMRI.

The second important aspect of the present study is the inclusion of MCI patients that both converted and did not convert to AD in addition to NA subjects and patients with overt AD. These intermediate classes are those in which a biomarker as FDG-PET can mostly help clinicians establish diagnosis and management. The common clinical challenge is not to distinguish NA subjects from patients with overt AD, but rather to discriminate among MCI patients those who will convert to AD from those who will not and possibly when (in which time range) they will convert. This challenge exist for both clinicians and neuropsychologists but also for the nuclear medicine physician due to frequent 'false positive' findings in visual FDG-PET reading, mainly due to atrophy or subcortical cerebrovascular pathology that lead to cortical disconnection phenomena.

The high analogy of the metabolic pattern of non-converters to that of NA - as expressed by the low AUC between the two classes - paves the way for a prognostic use for our statistical mechanistic model, especially considering the neat discrimination between ncMCI and converters. Hence, it is of utmost importance to be able to establish a significant prediction algorithm to link PET-based description of patients to their clinical severity. This step is crucial for shifting from a general description of the natural history of AD to a prospective diagnosis.

The smooth and progressive decrease of order of brain metabolism depicted in Fig. 1 confirms the idea that the spreading loss of integration across the brain is a crucial landmark of AD. Moreover, the capability of the degree of order of FDG-PET data to predict with a reasonable level of accuracy whether or not a conversion to dementia will occur after some years validates the present methodology and encourages the implementation of similar innovative ways of analyzing neuroimaging data in neurodegenerative disorders.

These findings furthermore highlight the relevance of FDG-PET for predicting conversion to dementia in MCI patients in the era of amyloid biomarkers since the presence of amyloidosis supports the presence of AD pathology but cannot accurately foresee if and when a subject with amyloidosis will eventually develop dementia.

Moreover, unlike multicenter studies, in this investigation diagnoses were very uniform in that they were performed by the same clinicians. All FDG-PET scans were also performed with the same camera. Therefore the likelihood that inhomogeneous subject samples and camera acquisitions could have impacted on data variability and results robustness is quite small. On the other hand, patients in the two groups of MCI converters and in the AD-dementia groups developed dementia when they were older than 65 ('late-onset Alzheimer dementia' LEOD) and they were all affected by amnesic syndrome. Therefore the present data especially reflect LEOD and may not be generalizable to early-onset AD patients in whom memory deficit can be milder and FDG-PET deficit more severely affects neocortical areas.

The general theoretical bases of our approach, can be understood from thermodynamics. The advantage of a thermodynamic-like approach resides in the possibility to get easy-to-use and generalizable statistical description (in our case the amount of variance explained by PC1) to appreciate the transformations of a complex system of which the mechanistic details are largely unknown (Mikulecky, 2001). It has to be noted that the largest eigenvalue of the between areas correlation, more than a network order index, must be intended as the first global thermodynamic measure of brain metabolism order. As a matter of fact the robustness and invariance to different partition, while surely favorable for global order estimation, are sub-optimal for specific network analyses that, in turn, ask for sensitivity to topological details. The use of the first eigenvalue of correlation matrix as global descriptor of order for different systems was first described in Gorban et al. (2010). More recently an fMRI investigation implementing the graph spectral entropy method in a psychiatric disorder (Sato et al., 2013) used eigenvalue/eigenvectors for the optimal spectral decomposition into modules (clusters) of the entire brain network built upon the mutual correlations among 351 ROIs. The authors applied a mathematical approach very similar to ours but focusing on the splitting of the brain network into Clusters while we focus on the generation of a global estimate of the amount of between ROIs correlation. What is remarkable in Sato et al. paper is the robustness of the four Cluster solution to different choices of patients. The robustness of eigenvector methods relies on the extreme redundance of between areas correlation matrix defining a system with relatively low effective dimensionality by means of an N(N-1)/2 distinct elements array (being N the number of ROIs). This robustness is still more evident (and more cogently related to our approach) in the results reported in Friston et al. (1993).

From thermodynamics we mutuated the ergodic hypothesis, originally set forth by Ludwig Boltzmann (Boltzmann, 1898) stating that the time spent by a system in some region of the phase space is proportional to the size of this region. A dynamic system is ergodic if, broadly speaking, it has the same behavior averaged over time as averaged over the space of all the system's states (phase space). The ergodic hypothesis is implicit in many computational physics studies. We assume that the average of a process parameter over time and the average over the statistical ensemble are the same. If the ergodic hypothesis holds true, the degree-of-order we measured in terms of correlation across patients of the same class, will give identical results of correlation between different time points of the same patient (within a time frame in which we can safely assume the practical invariance of disease status). The bootstrap approach can be considered as a first (albeit largely preliminary) step toward the validation of ergodic hypothesis.

The strong monotonic decrease we observed between the variance explained by the first component and time-to-conversion (Fig. 1) might lead to the possibility of a direct prognostic estimation of the degree of order of brain metabolism measured at the single patient level by means of consecutive PET scans. In principle, even a relatively small number of scans could prove useful thanks to the robustness of our statistical description, which summarizes the correlation network into a single metric.

In conclusion, the proposed methodology suggests a specific global connectivity-based biomarker able to identify AD pathology in its

various phases. The statistical mechanistic approach confirmed the network degeneration hypothesis and demonstrated for the first time by FDG-PET a progressive disruption of the giant component from NA to mild AD through different stages of cognitive impairment, including patients cognitively impaired but not converting to AD. If further validated, this statistical approach might provide a novel way to assess the functional networking status in patients and aid the clinician in foreseeing the evolution of mild cognitive impairment to overt dementia.

Supplementary data to this article can be found online at http://dx.doi.org/10.1016/j.neuroimage.2016.07.043.

Author contributions

MP, AG. and FN. designed the project. SM, ABr, DA, AP, MB and ABu recruited the patients and collected the data; MP, JÖ, AG, SM, ABr, DA, AP, MB, ABu and AC analyzed the data; MP and FN supervised the entire project. MP, AG, AC and FN wrote the paper with inputs from JÖ, SM and DA.

Competing financial interests

The authors declare no competing financial interests.

Acknowledgements

The authors wish to thank Professor Stone-Elander for the help in English editing.

References

Aisen, P.S., Petersen, R.C., Donohue, M.C., Gamst, A., Raman, R., Thomas, R.G., Walter, S., Trojanowski, J.Q., Shaw, L.M., Beckett, L.A., Jack Jr., C.R., Jagust, W., Toga, A.W., Saykin, A.J., Morris, J.C., Green, R.C., Weiner, M.W., Alzheimer's Disease Neuroimaging, I., 2010. Clinical core of the Alzheimer's disease neuroimaging initiative: progress and plans. Alzheimers Dement. 6, 239–246.

Boccaletti, S., Latora, V., Moreno, Y., Chavez, M., Hwang, D.U., 2006. Complex networks: structure and dynamics. Phys. Rep. 424, 175–308.

Boltzmann, L., 1898. Vorlesungen uber Gastheorie. Barth, J.A., Leipzig, Germany.

Bozzali, M., Parker, G.J., Serra, L., Embleton, K., Gili, T., Perri, R., Caltagirone, C., Cercignani, M., 2011. Anatomical connectivity mapping: a new tool to assess brain disconnection in Alzheimer's disease. NeuroImage 54, 2045–2051.

Bullmore, E., Sporns, O., 2009. Complex brain networks: graph theoretical analysis of structural and functional systems. Nat. Rev. Neurosci. 10, 186–198.

Canu, E., McLaren, D.G., Fitzgerald, M.E., Bendlin, B.B., Zoccatelli, G., Alessandrini, F., Pizzini, F.B., Ricciardi, G.K., Beltramello, A., Johnson, S.C., Frisoni, G.B., 2011. Mapping the structural brain changes in Alzheimer's disease: the independent contribution of two imaging modalities. J. Alzheimers Dis. 26 (Suppl. 3), 263–274.

Caroppo, P., Habert, M.O., Durrleman, S., Funkiewiez, A., Perlbarg, V., Hahn, V., Bertin, H., Gaubert, M., Routier, A., Hannequin, D., Deramecourt, V., Pasquier, F., Rivaud-Pechoux, S., Vercelletto, M., Edouart, G., Valabregue, R., Lejeune, P., Didic, M., Corvol, J.C., Benali, H., Lehericy, S., Dubois, B., Colliot, O., Brice, A., Le Ber, I., Predict, P.s.g., 2015. Lateral temporal lobe: an early imaging marker of the presymptomatic GRN disease? J. Alzheimers Dis. 47, 751–759.

Chandler, D., 1987. In: Chandler, D. (Ed.), Introduction to modern statistical mechanics. Oxford University Press, New York, USA.

Daianu, M., Jahanshad, N., Nir, T.M., Toga, A.W., Jack Jr., C.R., Weiner, M.W., Thompson, P.M., Alzheimer's Disease Neuroimaging, I., 2013. Breakdown of brain connectivity between normal aging and Alzheimer's disease: a structural k-core network analysis. Brain Connect 3, 407–422.

Damoiseaux, J.S., Rombouts, S.A., Barkhof, F., Scheltens, P., Stam, C.J., Smith, S.M., Beckmann, C.F., 2006. Consistent resting-state networks across healthy subjects. Proc. Natl. Acad. Sci. U. S. A. 103, 13848–13853.

Darroch, J.N., Mosimann, J.E., 1985. Canonical and principal components of shape. Biometrika 72, 241–252.

Della Rosa, P.A., Cerami, C., Gallivanone, F., Prestia, A., Caroli, A., Castiglioni, I., Gilardi, M.C., Frisoni, G., Friston, K., Ashburner, J., Perani, D., Consortium, E.-P., 2014. A standardized [^{18}F]-FDG-PET template for spatial normalization in statistical parametric mapping of dementia. Neuroinformatics 12, 575–593.

Di, X., Biswal, B.B., Alzheimer's Disease Neuroimaging, I., 2012. Metabolic brain covariant networks as revealed by FDG-PET with reference to resting-state fMRI networks. Brain Connect 2, 275–283.

Eguiluz, V.M., Chialvo, D.R., Cecchi, G.A., Baliki, M., Apkarian, A.V., 2005. Scale-free brain functional networks. Phys. Rev. Lett. 94, 018102.

Fischer, F.U., Wolf, D., Scheurich, A., Fellgiebel, A., Alzheimer's Disease Neuroimaging Initiative, 2015. Altered whole-brain white matter networks in preclinical Alzheimer's disease. Neurol. Clin. 8, 660–666.

Friston, K.J., Frith, C.D., Liddle, P.F., Frackowiak, R.S., 1993. Functional connectivity: the principal-component analysis of large (PET) data sets. J. Cereb. Blood Flow Metab. 13, 5–14.

Gardner, A., Astrand, D., Oberg, J., Jacobsson, H., Jonsson, C., Larsson, S., Pagani, M., 2014. Towards mapping the brain connectome in depression: functional connectivity by perfusion SPECT. Psychiatry Res. 223, 171–177.

Giuliani, A., Colafranceschi, M., Webber, C.L., Zbilut, J.P., 2001. A complexity score derived from principal components analysis of nonlinear order measures. Physica A 301, 567–588.

Gorban, A.N., Smirnova, E.V., Tyukina, T.A., 2010. Correlations, risk and crisis: from physiology to finance. Physica a-Statistical Mechanics and Its Applications 389, 3193–3217.

Gorelick, P.B., Scuteri, A., Black, S.E., Decarli, C., Greenberg, S.M., Iadecola, C., Launer, L.J., Laurent, S., Lopez, O.L., Nyenhuis, D., Petersen, R.C., Schneider, J.A., Tzourio, C., Arnett, D.K., Bennett, D.A., Chui, H.C., Higashida, R.T., Lindquist, R., Nilsson, P.M., Roman, G.C., Sellke, F.W., Seshadri, S., American Heart Association Stroke Council, C.o.E., Prevention, C.o.C.N.C.o.C.R., Intervention, Council on Cardiovascular, S., Anesthesia, 2011. Vascular contributions to cognitive impairment and dementia: a statement for healthcare professionals from the American Heart Association/American Stroke Association. Stroke 42, 2672–2713.

Hahn, K., Myers, N., Prigarin, S., Rodenacker, K., Kurz, A., Forstl, H., Zimmer, C., Wohlschlager, A.M., Sorg, C., 2013. Selectively and progressively disrupted structural connectivity of functional brain networks in Alzheimer's disease — revealed by a novel framework to analyze edge distributions of networks detecting disruptions with strong statistical evidence. NeuroImage 81, 96–109.

Huang, C., Eidelberg, D., Habeck, C., Moeller, J., Svensson, L., Tarabula, T., Julin, P., 2007. Imaging markers of mild cognitive impairment: multivariate analysis of CBF SPECT. Neurobiol. Aging 28, 1062–1069.

Ishii, K., Soma, T., Kono, A.K., Sofue, K., Miyamoto, N., Yoshikawa, T., Mori, E., Murase, K., 2007. Comparison of regional brain volume and glucose metabolism between patients with mild dementia with lewy bodies and those with mild Alzheimer's disease. J. Nucl. Med. 48, 704–711.

Iturria-Medina, Y., Evans, A.C., 2015. On the central role of brain connectivity in neurodegenerative disease progression. Front. Aging Neurosci. 7, 90.

Jolicoeur, P., Mosimann, J.E., 1960. Size and shape variation in the painted turtle. A principal component analysis. Growth 24, 339–354.

Jolliffe, I.T., 2002. In: Jolliffe, I.T. (Ed.), Principal component analysis and factor analysis. Springer Verlag, New York, USA.

Lee, D.S., Kang, H., Kim, H., Park, H., Oh, J.S., Lee, J.S., Lee, M.C., 2008. Metabolic connectivity by interregional correlation analysis using statistical parametric mapping (SPM) and FDG brain PET; methodological development and patterns of metabolic connectivity in adults. Eur. J. Nucl. Med. Mol. Imaging 35, 1681–1691.

Liu, Z., Zhang, Y., Yan, H., Bai, L., Dai, R., Wei, W., Zhong, C., Xue, T., Wang, H., Feng, Y., You, Y., Zhang, X., Tian, J., 2012. Altered topological patterns of brain networks in mild cognitive impairment and Alzheimer's disease: a resting-state fMRI study. Psychiatry Res. 202, 118–125.

Loeb, C., Gandolfo, C., 1983. Diagnostic evaluation of degenerative and vascular dementia. Stroke 14, 399–401.

McKhann, G.M., Knopman, D.S., Chertkow, H., Hyman, B.T., Jack Jr., C.R., Kawas, C.H., Klunk, W.E., Koroshetz, W.J., Manly, J.J., Mayeux, R., Mohs, R.C., Morris, J.C., Rossor, M.N., Scheltens, P., Carrillo, M.C., Thies, B., Weintraub, S., Phelps, C.H., 2011. The diagnosis of dementia due to Alzheimer's disease: recommendations from the National Institute on Aging-Alzheimer's Association workgroups on diagnostic guidelines for Alzheimer's disease. Alzheimers Dement. 7, 263–269.

Mikulecky, D.C., 2001. Network thermodynamics and complexity: a transition to relational systems theory. Comput. Chem. 25, 369–391.

Morbelli, S., Drzezga, A., Perneczky, R., Frisoni, G.B., Caroli, A., van Berckel, B.N., Ossenkoppele, R., Guedj, E., Didic, M., Brugnolo, A., Sambuceti, G., Pagani, M., Salmon, E., Nobili, F., 2012. Resting metabolic connectivity in prodromal Alzheimer's disease. A European Alzheimer Disease Consortium (EADC) project. Neurobiol. Aging 33, 2533–2550.

Nobili, F., Brugnolo, A., Calvini, P., Copello, F., De Leo, C., Girtler, N., Morbelli, S., Piccardo, A., Vitali, P., Rodriguez, G., 2005. Resting SPECT-neuropsychology correlation in very mild Alzheimer's disease. Clin. Neurophysiol. 116, 364–375.

Nobili, F., Salmaso, D., Morbelli, S., Girtler, N., Piccardo, A., Brugnolo, A., Dessi, B., Larsson, S.A., Rodriguez, G., Pagani, M., 2008. Principal component analysis of FDG PET in amnestic MCI. Eur. J. Nucl. Med. Mol. Imaging 35, 2191–2202.

Pagani, M., Salmaso, D., Rodriguez, G., Nardo, D., Nobili, F., 2009. Principal component analysis in mild and moderate Alzheimer's disease—a novel approach to clinical diagnosis. Psychiatry Res. 173, 8–14.

Pagani, M., Chio, A., Valentini, M.C., Oberg, J., Nobili, F., Calvo, A., Moglia, C., Bertuzzo, D., Morbelli, S., De Carli, F., Fania, P., Cistaro, A., 2014. Functional pattern of brain FDG-PET in amyotrophic lateral sclerosis. Neurology 83, 1067–1074.

Pagani, M., De Carli, F., Morbelli, S., Oberg, J., Chincarini, A., Frisoni, G.B., Galluzzi, S., Perneczky, R., Drzezga, A., van Berckel, B.N., Ossenkoppele, R., Didic, M., Guedj, E., Brugnolo, A., Picco, A., Arnaldi, D., Ferrara, M., Buschiazzo, A., Sambuceti, G., Nobili, F., 2015. Volume of interest-based [^{18}F]fluorodeoxyglucose PET discriminates MCI converting to Alzheimer's disease from healthy controls. A European Alzheimer's Disease Consortium (EADC) study. NeuroImage Clin. 7, 34–42.

Pagani, M., Öberg, J., De Carli, F., Calvo, A., Moglia, C., Canosa, A., Nobili, F., Morbelli, S., Fania, P., Cistaro, A., Chiò, A., 2016. Metabolic connectivity in amyotrophic lateral sclerosis as revealed by independent component analysis. Hum. Brain Mapp. 37, 942–953.

Petersen, R.C., Negash, S., 2008. Mild cognitive impairment: an overview. CNS Spectr. 13, 45–53.

Picco, A., Polidori, M.C., Ferrara, M., Cecchetti, R., Arnaldi, D., Baglioni, M., Morbelli, S., Bastiani, P., Bossert, I., Fiorucci, G., Brugnolo, A., Dottorini, M.E., Nobili, F., Mecocci, P., 2014. Plasma antioxidants and brain glucose metabolism in elderly subjects with cognitive complaints. Eur. J. Nucl. Med. Mol. Imaging 41, 764–775.

Rombouts, S.A., Damoiseaux, J.S., Goekoop, R., Barkhof, F., Scheltens, P., Smith, S.M., Beckmann, C.F., 2009. Model-free group analysis shows altered BOLD FMRI networks in dementia. Hum. Brain Mapp. 30, 256–266.

Sato, J.R., Takahashi, D.Y., Hoexter, M.Q., Massirer, K.B., Fujita, 2013. A. Measuring network's entropy in ADHD: a new approach to investigate neuropsychiatric disorders. NeuroImage 77, 44–51.

Scheffer, M., Carpenter, S.R., Lenton, T.M., Bascompte, J., Brock, W., Dakos, V., van de Koppel, J., van de Leemput, I.A., Levin, S.A., van Nes, E.H., Pascual, M., Vandermeer, J., 2012. Anticipating critical transitions. Science 338, 344–348.

Seeley, W.W., Crawford, R.K., Zhou, J., Miller, B.L., Greicius, M.D., 2009. Neurodegenerative diseases target large-scale human brain networks. Neuron 62, 42–52.

Sethi, S.P., 1971. Comparative cluster analysis for world markets. J. Mark. Res. 8, 348–354.

Smith, S.M., Fox, P.T., Miller, K.L., Glahn, D.C., Fox, P.M., Mackay, C.E., Filippini, N., Watkins, K.E., Toro, R., Laird, A.R., Beckmann, C.F., 2009. Correspondence of the brain's functional architecture during activation and rest. Proc. Natl. Acad. Sci. U. S. A. 106, 13040–13045.

Soofi, E.S., 1994. Capturing the intangible concept of information. Journ. Am. Stat. Ass. 89, 1243–1254.

Sorg, C., Riedl, V., Muhlau, M., Calhoun, V.D., Eichele, T., Laer, L., Drzezga, A., Forstl, H., Kurz, A., Zimmer, C., Wohlschlager, A.M., 2007. Selective changes of resting-state networks in individuals at risk for Alzheimer's disease. Proc. Natl. Acad. Sci. U. S. A. 104, 18760–18765.

Spetsieris, P.G., Ko, J.H., Tang, C.C., Nazem, A., Sako, W., Peng, S., Ma, Y., Dhawan, V., Eidelberg, D., 2015. Metabolic resting-state brain networks in health and disease. Proc. Natl. Acad. Sci. U. S. A. 112, 2563–2568.

Stepan-Buksakowska, I., Szabo, N., Horinek, D., Toth, E., Hort, J., Warner, J., Charvat, F., Vecsei, L., Rocek, M., Kincses, Z.T., 2014. Cortical and subcortical atrophy in Alzheimer disease: parallel atrophy of thalamus and hippocampus. Alzheimer Dis. Assoc. Disord. 28, 65–72.

Sun, Y., Yin, Q., Fang, R., Yan, X., Wang, Y., Bezerianos, A., Tang, H., Miao, F., Sun, J., 2014. Disrupted functional brain connectivity and its association to structural connectivity in amnestic mild cognitive impairment and Alzheimer's disease. PLoS One 9, e96505.

Tan, Y.J., Oliveberg, M., Fersht, A.R., 1996. Titration properties and thermodynamics of the transition state for folding: comparison of two-state and multi-state folding pathways. J. Mol. Biol. 264, 377–389.

Tzourio-Mazoyer, N., Landeau, B., Papathanassiou, D., Crivello, F., Etard, O., Delcroix, N., Mazoyer, B., Joliot, M., 2002. Automated anatomical labeling of activations in SPM using a macroscopic anatomical parcellation of the MNI MRI single-subject brain. NeuroImage 15, 273–289.

van den Heuvel, M.P., Stam, C.J., Kahn, R.S., Hulshoff Pol, H.E., 2009. Efficiency of functional brain networks and intellectual performance. J. Neurosci. 29, 7619–7624.

Varrone, A., Asenbaum, S., Vander Borght, T., Booij, J., Nobili, F., Nagren, K., Darcourt, J., Kapucu, O.L., Tatsch, K., Bartenstein, P., Van Laere, K., European Association of Nuclear Medicine Neuroimaging, 2009. EANM procedure guidelines for PET brain imaging using [^{18}F]FDG, version 2. Eur. J. Nucl. Med. Mol. Imaging 36, 2103–2110.

Wahlund, L.O., Barkhof, F., Fazekas, F., Bronge, L., Augustin, M., Sjogren, M., Wallin, A., Ader, H., Leys, D., Pantoni, L., Pasquier, F., Erkinjuntti, T., Scheltens, P., European Task Force on Age-Related White Matter, 2001. A new rating scale for age-related white matter changes applicable to MRI and CT. Stroke 32, 1318–1322.

Wang, K., Liang, M., Wang, L., Tian, L., Zhang, X., Li, K., Jiang, T., 2007. Altered functional connectivity in early Alzheimer's disease: a resting-state fMRI study. Hum. Brain Mapp. 28, 967–978.

Yi, H.A., Moller, C., Dieleman, N., Bouwman, F.H., Barkhof, F., Scheltens, P., van der Flier, W.M., Vrenken, H., 2016. Relation between subcortical grey matter atrophy and conversion from mild cognitive impairment to Alzheimer's disease. J. Neurol. Neurosurg. Psychiatry 87, 425–432.